Dual-band THz 2×2 MIMO antenna array for THz wireless communication networks

POONAM KOUNDAL[1,*], SIMRANJIT SINGH[2], RAJBIR KAUR[1]
[1]*Punjabi University Patiala, Punjab, India*
[2]*Punjab Engineering College (Deemed to be University), Chandigarh, India*

A single rectangular microstrip antenna is developed for wireless applications, along with a 2×2 Multiple Input Multiple Output (MIMO) antenna array. The substrate is formed out of polyimide material, having an electrical dielectric constant of 3.5 and a thickness of 0.04 mm. An extremely small rectangular patch antenna with measurements of 0.075 mm by 0.11 mm by 0.04 mm is employed in the proposed MIMO antenna array. For the resonating frequency, performance metrics such as reflection coefficient, efficiency, bandwidth, peak gain, antenna directivity, and VSWR are computed. The intended MIMO array has a reflection coefficient of less than -10 dB and resonates for two different frequencies: 0.7638 THz, and 1.0804 THz. The developed MIMO array has a maximum possible antenna gain and directivity of 12.30 dB and 12.33 dB respectively, maximum radiation efficiency of 90% and VSWR below 2 for the resonant frequency. Moreover, the MIMO parameters for also observed, such as ECC being 0.0008, diversity gain being 9.9999 dB, CCL being 0.44 and 0.42, MEG being -2 to 0 dB and TARC being below -20 dB.

(Received December 29, 2023; accepted October 2, 2024)

Keywords: Microstrip patch antenna, MIMO antenna array, THz band

1. Introduction

Wireless communication has made enormous advancements in recent years, leading to the current fifth-generation (5G) wireless networks. The typical data speeds that 5G networks can deliver are as much as 100 times quicker than those of the existing 4G networks [1,2]. For 5G, the progress of the system design's performance is greatly aided by the antenna array. An antenna array is made up of numerous antennas working together to produce certain performance parameters. Such antenna arrays are utilised in many applications, including radio astronomy, wireless communications, and radar communication. Antenna arrays provide many advantages over single antennae, including increased gain, excellent directionality, and beamforming [3,4].

With the rapid advancement of technology, wireless networking is becoming more and more significant. This situation has led to a sharp increase in internet traffic, which has led to a shortage of bandwidth as well as associated resources. Considering the data rate, which is approaching Gbps and could perhaps exceed Tbps given the present traffic demand. Data rates of up to Gbps are possible with today's most advanced THz communication networks [5]. Thus, the most practical method for increasing the data transmission rate may be to use the THz frequency spectrum, which is the empty region between microwave as well as infrared light. Wide bandwidth for greater data rates, dramatically improved directivity, a low level of interference, and system layout compactness are just a few of the advantages that the frequency bands above the microwave spectrum provide for wireless networks of communication. This happens because the antenna sizes get very tiny at the THz frequency [6]. The frequency range and wavelength range for this region of the electromagnetic spectrum are 0.1 to 10 THz and 0.03 to 0.3 mm, respectively shown in Fig. 1. Numerous applications that call for high data rates were made available by the THz band's large bandwidth, with a bandwidth greater than 10 GHz [7,8].

The THz frequency spectrum contains characteristics of both light waves and millimetre frequency waves. The THz frequency range has a wider bandwidth and an intensely directional beam than millimeter-wave and is more effective and penetrating instead of light waves. THz antennas provide numerous advantages, however there additionally exist many design challenges. The size of the antenna is dramatically reduced at high frequency. There is an inserting restriction for THz antennas. Another design difficulty for THz antennas is their effective radiation [9].

THz communication is one of the essential technologies for upcoming 6G wireless networks since it can support extraordinarily rapid data transfer and a dozen GHz of bandwidth [10]. Despite this, communications using THz suffer from significant path loss due to the very high- frequency [11,12]. A more broad and consistent communication footprint is provided by the implementation of MIMO, which increases the coverage area and connectivity of wireless networks [13]. Moreover, MIMO technology, which somewhat can provide highly directional beams with huge antenna array gain, may be used in upcoming THz communications to compensate for the significant path loss. Additionally, a research investigation has demonstrated that MIMO technology can

boost spectrum efficiency while reducing energy consumption in wireless communications applications about 10–20 times [14,15].

Many academic researchers have been concentrating on the newest THz frequency band spectrum in recent years. Many researchers have worked on small-sized antenna designs for THz frequency. M. Singh et al. [16] designed an ultra-wideband THz MIMO design by utilizing the polyimide substrate with a 3.5 dielectric constant and 50 µm height. This designed MIMO resonates for two frequencies 0.6 THz and 0.8 THz with the return loss of -23.9 dB and -29.2 dB respectively. Moreover, this designed MIMO offers a gain of 8.28 dB, a directivity of 9.7 dB of directivity, and an ECC of 0.01.

Rashmi Pant and Malviya Leeladhar [17] proposed a MIMO array for THz frequency having the measurements of 1200 µm × 2200 µm × 191.29 µm. This MIMO array offers an antenna gain of 11.3 dB, an antenna efficiency of 66.4%, an impedance bandwidth of 0.04 THz and lower than -10 dB return loss. Moreover, they analysed the MIMO parameters such as ECC of 2.8×10^{-6}, diversity of 9.9 dB and CCL lower than 0.4bps/Hz.

S. M. et al. Shamim (2023) [18] designed a high-speed antenna utilizing graphene that operates at 2.96 THz frequency for wireless network applications. To achieve the desired values, various parameters are investigated parametrically. For 2.96 THz resonance frequency, this antenna offers a minimal reflection coefficient of -50.98 dB, VSWR of 1.02, gain of 5.4 dB, and bandwidth of 27 GHz. All of the simulations were performed employing the finite integration technique and CST software.

Gaofang Li et al. [19] present a triple-band microstrip antenna for THz frequency utilizing a photonic band gap substrate. The polyimide and photonic band gap substrates combined to form a multilayer structure that allowed the antenna to operate in multiple bands. the presented antenna for the resonant frequency offers a high antenna gain of 7.66 dB and also a radiation efficiency of 91%.

Waleed S. et al. [20] present the dual-band array for THz frequency which offers lower return loss of -20dB and -23 dB for the resonance frequencies of 0.708 THz and 0.752 THz. Additionally, it provides a peak gain of 24 dB, high directivity of 24.4 dB, antenna efficiency of 95%, a bandwidth of 4.7 GHz and VSWR lies 1 to 2. However, this array encounters several challenges and has a smaller bandwidth.

Kushwaha et al. [21] present a dual-band THz antenna by using a polyimide substrate for THz network applications. This antenna offers a higher antenna gain of 7.91 dB, directivity of 8.61, VSWR close to one and maximum bandwidth of 36.25 GHz. Moreover, it offers -10 dB impedance for the resonating frequency range of 0.615 THz and 0.651 THz. And thus, can be used for characterization areas.

It is evident from the aforementioned explanation that the proposed MIMO array performs better than the previous THz antenna. The proposed MIMO provides greater antenna bandwidth with extremely better performance. Moreover, the majority of researchers have only developed a single THz antenna, and haven't yet determined the ideal configuration for a MIMO array. Furthermore, the majority of researchers have only developed a single THz antenna, and haven't yet determined the ideal configuration for a MIMO array. The division of this research study into many sections is explained below. The design configuration, parametric analysis and result analysis for the single-patch antenna are described in Section 2. The design modelling of a proposed 2×2 MIMO for THz frequency is discussed in Section 3. Additionally, a detailed summary of the entire work done is described in the concluding section.

2. Design configuration and results for a single rectangular patch antenna

2.1. Single antenna geometry

A single microstrip antenna must be evaluated at the initial phase. For simulating the patch antenna, the substrate material and resonating frequency were determined. High-frequency structure simulator (HFSS) software is used to design this patch antenna, which is an element of the proposed MIMO antenna array. A patch antenna has a wide range of uses and can be shaped like a square shape, circular, or rectangular shape. The ground is the lowest layer in a microstrip patch antenna, whereas the patch element is the uppermost layer of the substrate.

To determine the dimensions of the microstrip patch antenna the following equations are used [22, 23]. The patch's length and width can be determined by using equations (1-2):

$$L = \frac{(2N+1)}{\sqrt{\varepsilon_{reff}}} \times \frac{\lambda}{2} - 2\Delta L \quad (1)$$

$$W = \frac{(2N+1)}{\sqrt{\frac{\varepsilon_r + 1}{2}}} \times \frac{\lambda}{2} \quad (2)$$

where, ε_{reff}: effective refractive index, ε_r: dielectric constants and N: integer.

To minimize the surface wave effect in the printed circuit board, the upper limit of substrate thickness h may also be determined using the following equation.

The height of the substrate (h) can be calculated by using equation (3).

$$h = \frac{\lambda}{4\sqrt{\varepsilon_r}} \quad (3)$$

Since the dielectric characteristics of the substrate material differ from that of the air, the effective dielectric constant must be computed. This can be computed by using equation (4).

$$\varepsilon_{reff} = \frac{\varepsilon_r + 1}{2} + \frac{\varepsilon_r - 1}{2}\left[1 + 12\,\frac{h}{w}^{-\frac{1}{2}}\right] \quad (4)$$

Because of the fringing effect, the size of the patch antenna increases by ΔL. The real length of the patch can be calculated with the help of equation (5).

$$\Delta L = 0.412\ h\ \frac{(\varepsilon_{reff}+0.3)(\frac{w}{h}+0.264)}{(\varepsilon_{reff}+0.258)(\frac{w}{h}+0.8)} \quad (5)$$

The feedline's length F_l and feedline's width F_w for 50- ohm transmission line can be calculated with equations (6-7).

$$F_l = (2M+1)\times\frac{\lambda}{2} \quad (6)$$

$$F_w = \frac{1}{0.8}\left[\frac{9.5138h}{e\sqrt{\lambda(\varepsilon_{reff}+1.41)/w}} - t\right] \quad (7)$$

where, M: integer.

Table 1. Dimensions for simulated antenna

Antenna Parameters	Dimensions
P_w (Patch's Width)	0.11 mm
P_l (Patch's Length)	0.075 mm
S_w (Substrate's Width)	0.22 mm
S_l (substrate's Length)	0.22 mm
F_w (Feedline's Width)	0.03 mm
F_l (Feedline's Length)	0.06 mm
h (Substrate's Height)	0.04 mm

The dimensions of the substrate and ground are identical. The following equations (8-9) are used to determine the ground's L_g and ground's width W_g (Muhammad I. K. et al. 2020).

$$L_g = 6h + L \quad (8)$$

$$W_g = 6h + W \quad (9)$$

The parameters used for this designed patch antenna are shown in Table 1.

2.2. Parametric analysis of microstrip antenna

To achieve the appropriate performance metrics, a parametric analysis of the patch antenna is carried out, which involves the study of various parameters of the patch antenna. the performance of an antenna is greatly influenced by the antenna elements' physical arrangement and geometry. By varying the dimensions of the radiating patch, the substrate's height, and the ground plane's dimensions can optimize the antenna's performance. The geometrical characteristics of the microstrip patch antenna are created utilizing a precise parametric analysis. The following are the significant parameters that we have taken into account for the analysis:

A. The Ground Plane

The measurements of the ground plane are taken into account to achieve the desired bandwidth as well as appropriate antenna return loss. The length of the ground (G_L) and the width of the ground plane (G_W) are both the same and increase gradually from 0.19 mm to 0.22 mm. The return loss and antenna bandwidth are optimized with a 0.01 mm step size of the ground plane's dimensions as shown in Fig. 1. The varying dimension of the ground plane greatly affects both antenna bandwidth as well as return loss. The optimal antenna performance of the designed antenna is achieved at 0.22 mm dimensions of ground.

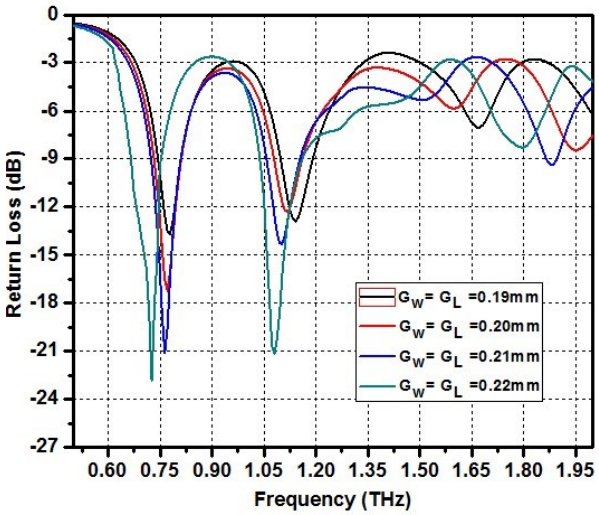

Fig. 1. The impact of expanding the measurements of the ground plane on the designed antenna (color online)

B. The height of substrate

Fig. 2 illustrates the return loss of the designed patch antenna for the various polyimide substrate heights (h) which vary from 0.01 mm to 0.05 mm. This figure shows that the greater return loss for the designed antenna is achieved at h= 0.03 mm as compared to other height dimensions. Hence, 0.03 mm is the optimal height with minimal return loss for the designed antenna.

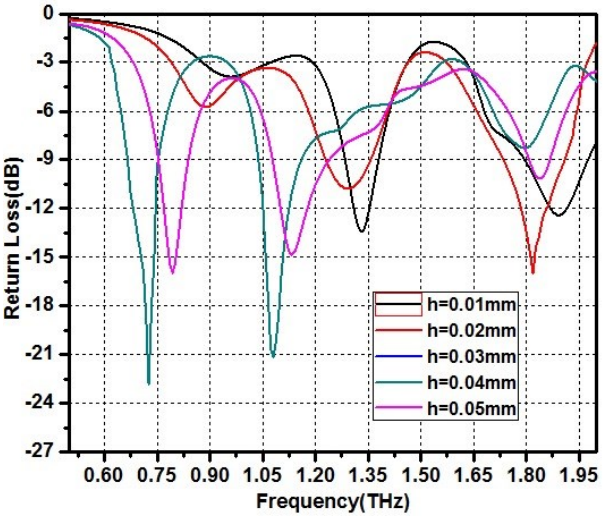

Fig. 2. The impact of expanding the height of the substrate for designed antenna (color online)

C. The location of the microstrip feedline

To ensure the best impedance match and raise the antenna's characteristic impedance, a 0.03 mm wide microstrip feedline is utilised, resulting in increased radiation efficiency and higher antenna gain. The location of the microstrip feedline is shifted by step size 0.02 mm from the centre to the right and, finally, to the left-hand side. Fig. 3 illustrates the analysed results for these locations of the microstrip feedline.

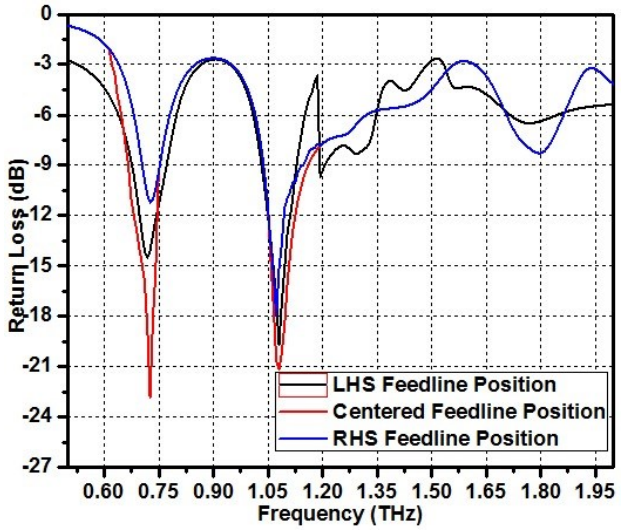

Fig. 3. The impact of the position of the feedline on the designed antenna (color online)

These results show that by moving the feedline location by 0.02 mm toward the left side, a moderate bandwidth as well as return loss and low efficiency are achieved. Additionally, at the resonant frequencies, similar performance metrics for the right side were noted to be lowering. On the other hand, better return loss, increased bandwidth, and enhanced efficiency were attained at the centre position of the microstrip feedline, considering the optimal feedline location of the ideal antenna.

2.3. Design procedure and result analysis of single patch antenna

In this section, the rectangular antenna is transformed into a hexagonal slot patch antenna. Firstly, a rectangular antenna for THz frequency is designed by using mathematical equations (1- 6). Fig. 4(a) illustrates the designed rectangular microstrip antenna having polyimide substrate material with a 3.4 dielectric constant. To further increase the performance of this designed antenna, a hexagonal slot with a dimension of 0.04 mm is cut into the radiating patch element shown in Fig. 4(b). Moreover, Fig. 4(c) shows the ground of the designed single microstrip antenna. The rectangular radiating patch has measurements of 0.075 mm × 0.11 mm × 0.04 mm. The substrate layer is placed between the radiating patch and the ground plane.

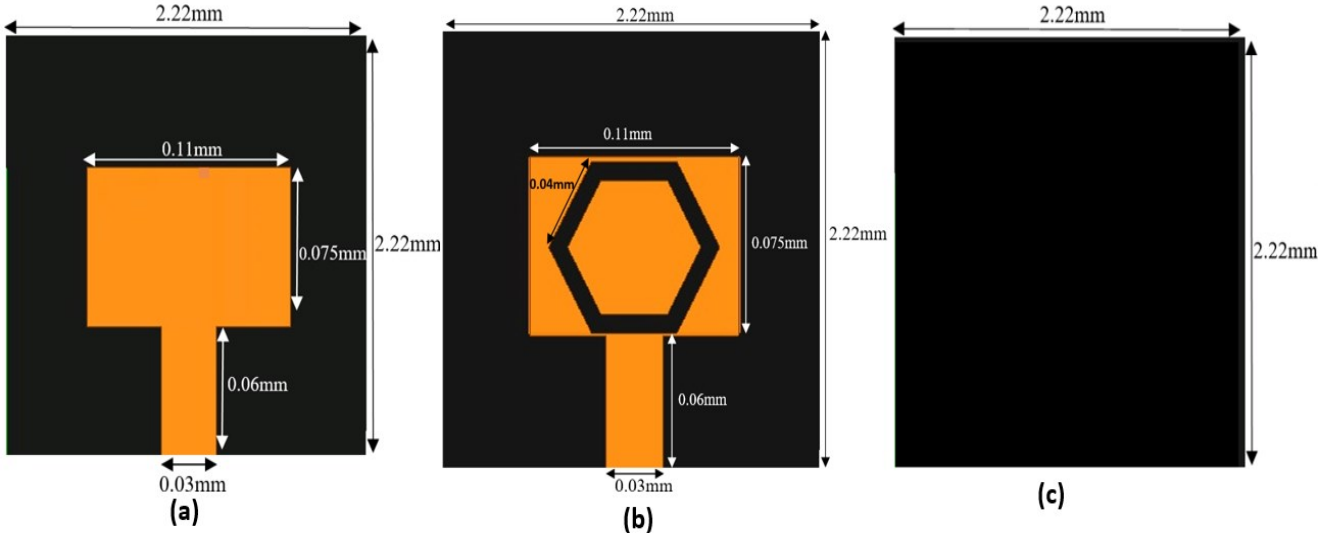

Fig. 4. Design of single rectangular patch antenna (color online)

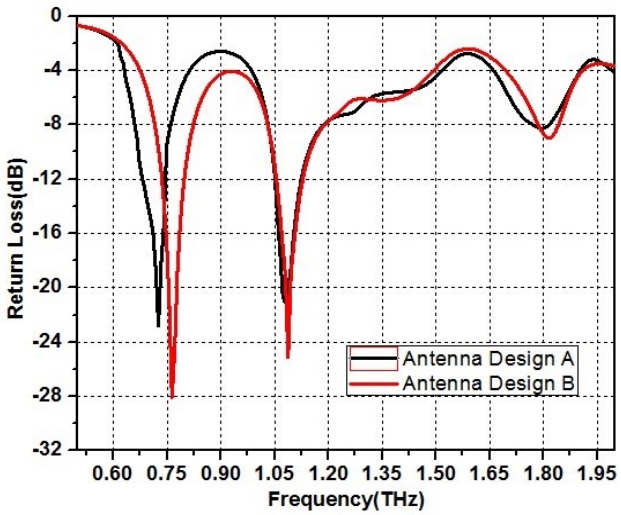

Fig. 5. Reflection coefficient of single patch antenna A and B (color online)

After observing the performance of antennae A and B, it is noticed that their respective return losses are below -10 dB. Moreover, antenna gain, impedance bandwidth, directivity, VSWR and antenna efficiency are also taken into consideration. In Fig. 5 the return loss for both antennae A and B are shown which defines the effective antenna impedance match with a certain bandwidth.

The rectangular antenna 'A' has a return loss of -22.8341 dB, and -21.1270 dB at 0.7261 THz and 1.0804 THz resonating frequencies respectively. Additionally, Antenna 'B' resonates at 0.7638 THz and 1.0879 THz with the return loss of -28.0939 dB and -25.1371 dB respectively. Moreover, the observed maximum bandwidth for Antenna 'A' and 'B' is 81.3 GHz and 103.9 dB respectively. Fig. 6 illustrates the antenna gain for designed antennas 'A' and 'B'. The obtained gain for antenna A is 7.31 dB, whereas the improved gain of antenna B is 9.16 dB. Similarly, the obtained directivity for antenna A is 7.31 dB, whereas the improved directivity of antenna B is 9.17 dB as appears in Fig. 7. Furthermore, the VSWR for antennae A and B lies between 1 and 2, as appears in Fig. 8 and the efficiency for antennae A and B is 86% and 88% respectively as shown in Fig. 9.

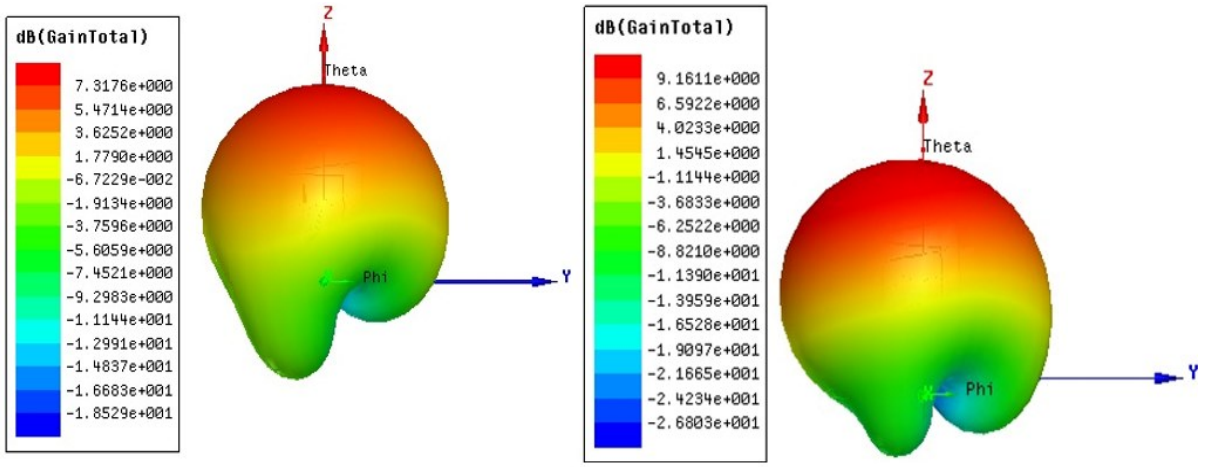

a) b)

Fig. 6. 3D view of gain for antenna A and B (color online)

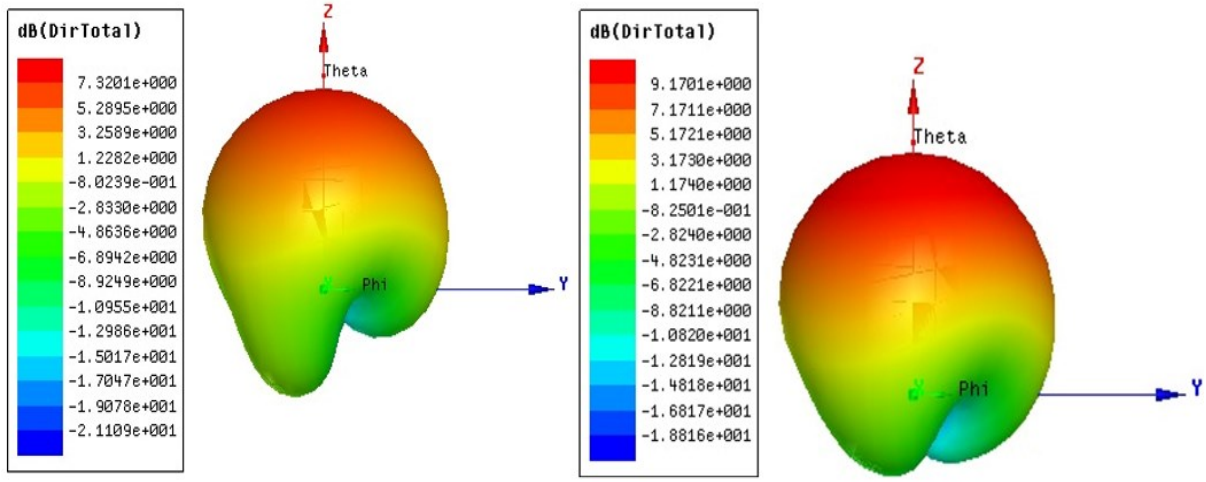

a) b)

Fig. 7. 3D view of directivity for antenna A and B (color online)

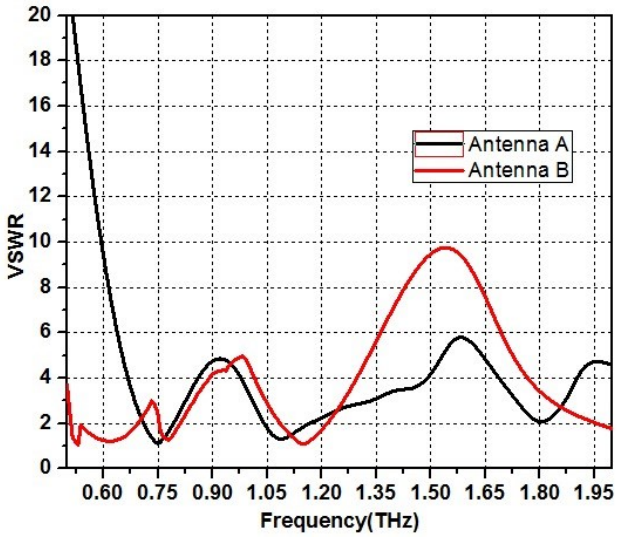

Fig. 8. VSWR of single patch antenna A and B (color online)

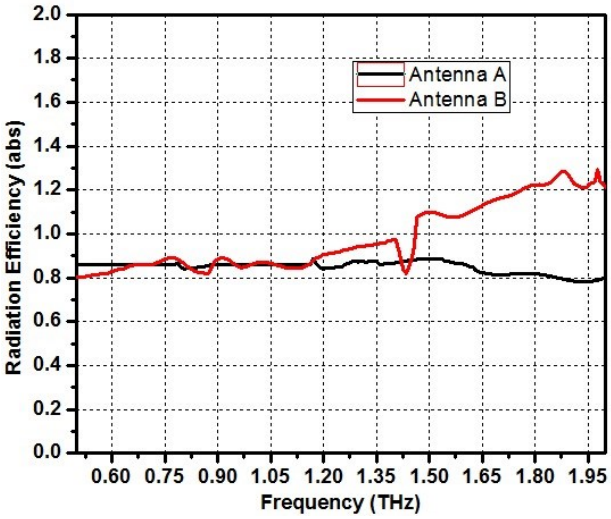

Fig. 9. Radiation efficiency of single patch antenna (color online)

3. 4-Element MIMO antenna array for THz applications

MIMO is the greater choice for high-speed wireless applications since it provides better performance parameters. In this section, Fig. 10 demonstrates the simulated 2×2 MIMO antenna array which comes after the development of slotted single patch antenna B. Hexagonal-slotted antenna B is used to develop the proposed THz MIMO array. The polyimide substrate material is used in the proposed array with the dimensions of 0.44 mm × 0.44 mm × 0.04 mm. Four patch elements of identical dimensions are employed in 2×2 MIMO to strengthen the overall performance of the antenna system.

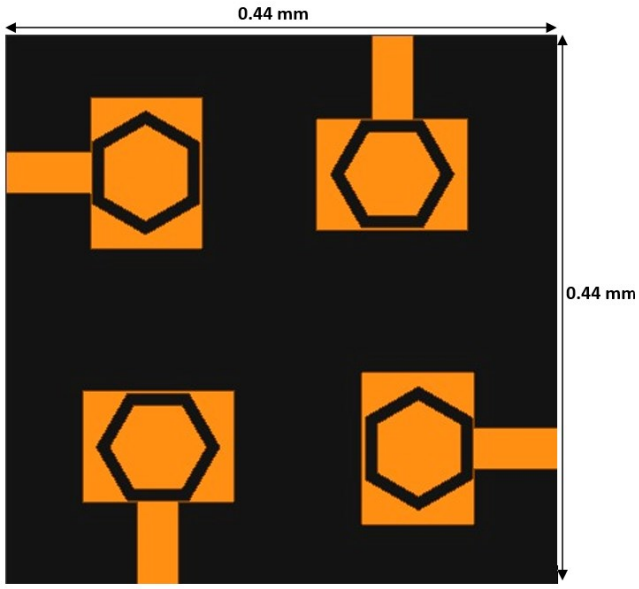

Fig. 10. 2×2 MIMO antenna array (color online)

Because of the very high THz frequency, the size of the proposed array is very compact. The wider bandwidth and higher data rate are the main characteristics of the higher-frequency MIMO array. The wider bandwidth fulfils the requirement for high-speed data networks. The antenna performance parameters such as gain, bandwidth, return loss, antenna directivity and VSWR are evaluated. After evaluation, it is clear that the performance parameters of the proposed MIMO antenna array are much enhanced than the designed single-patch antennas.

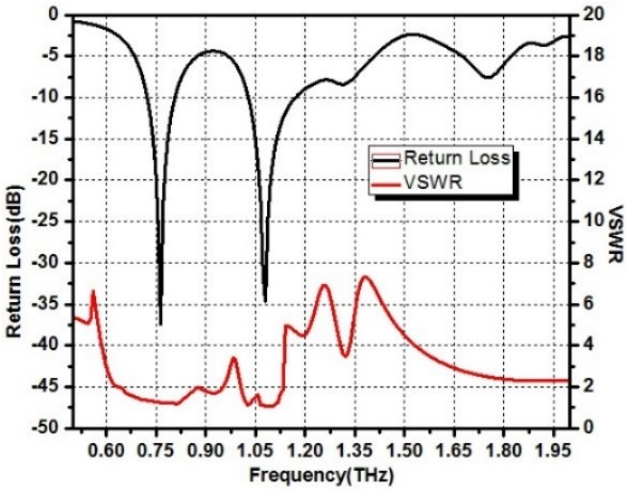

Fig. 11. Return loss and VSWR of 2×2 MIMO (color online)

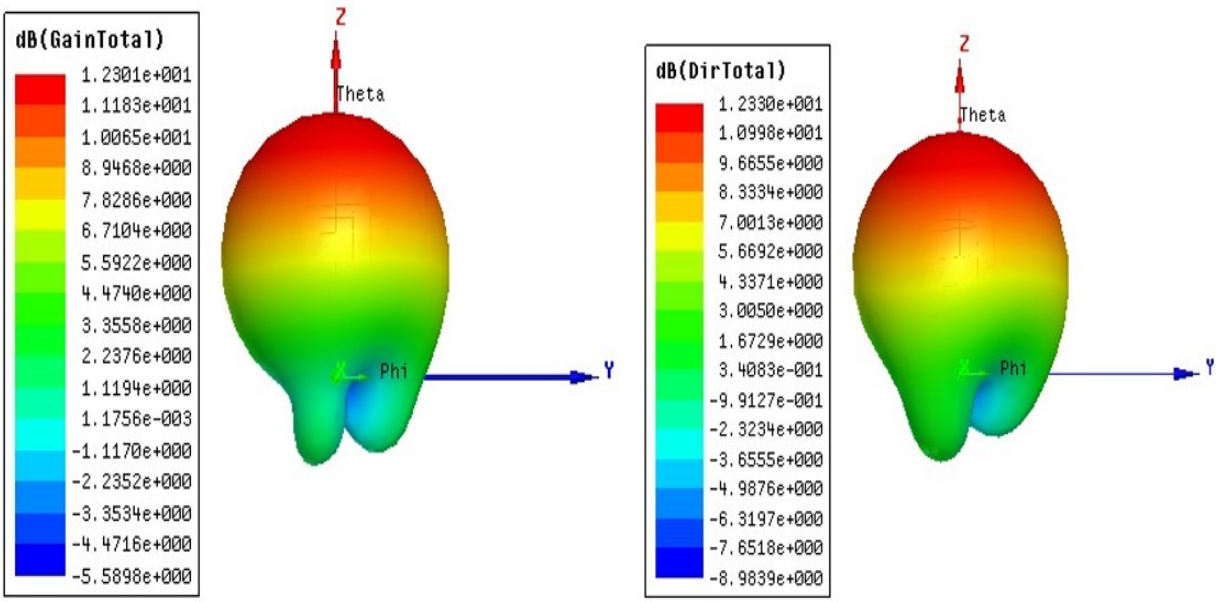

Fig. 12. Gain and directivity of 2×2 MIMO (color online)

The proposed 2×2 MIMO has a larger bandwidth of 170.3 GHz and resonates for dual frequencies that are 0.7638 THz, and 1.0804 THz with a return loss of –-37.4166 dB and 34.6443 dB respectively. Moreover, the proposed array offers a higher gain of 12.30 dB as well as a higher directivity of 12.33 dB as shown in Fig. 11. Furthermore, the proposed array for resonating frequencies has the VSWR which lies between 1 and 2 i.e. 1.2280 and 1.0786 and the radiating efficiency of 90%.

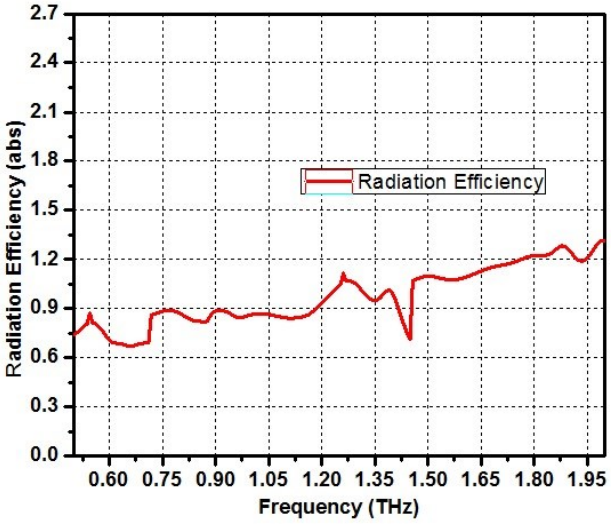

Fig. 13. Radiation efficiency for MIMO Array (color online)

Furthermore, to reduce the mutual coupling among antenna ports, the transmission coefficients of 4-ports of proposed 2×2 MIMO in terms of S23, S12, S24, S33, S34 and S14 are analysed and illustrated in Fig. 14. The analysed result shows that the achieved isolation among the 4-port of the proposed MIMO is lesser than -10 dB.

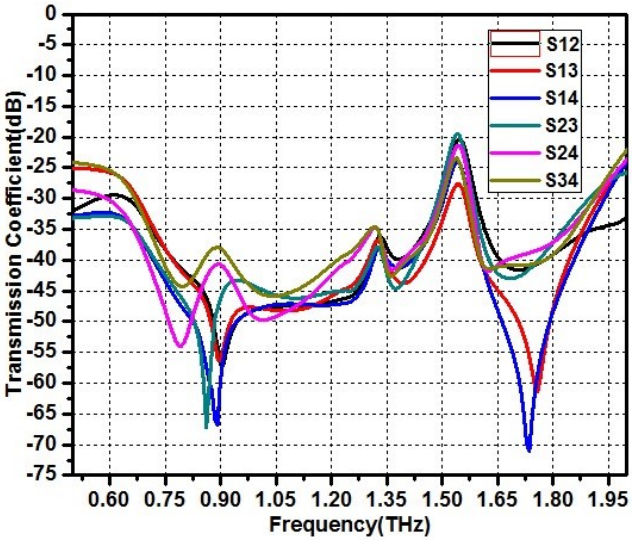

Fig. 14. Port isolation for 2×2 MIMO (color online)

Additionally, the MIMO performance parameters including Envelope correlation coefficient (ECC), Channel Capacity Loss (CCL), diversity gain, Total Active Reflection Coefficient (TARC) and Mean Effective Gain (MEG) are analysed. Fig. 15 shows simulated ECC as well as Diversity Gain of the proposed MIMO array. For the THz resonating frequencies, ECC is 0.0008 and Diversity Gain is 9.9999 dB.

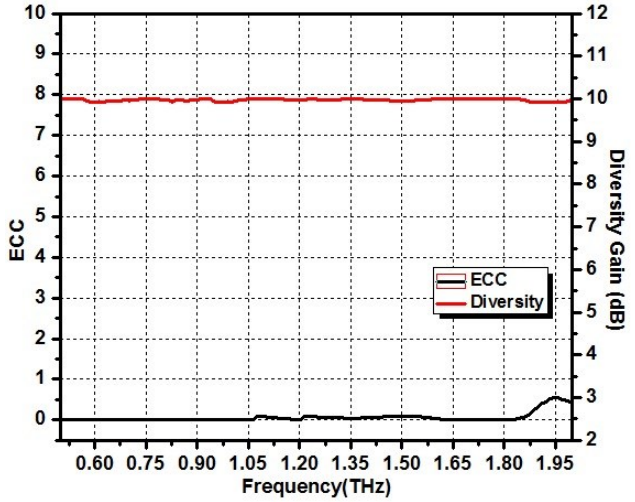

Fig. 15. ECC and diversity of 2×2 MIMO (color online)

The optimal value for CCL is 0.5 bits/s/Hz and it occurs due to correlation effects. However, the values near to 0.5 bits/s/Hz may also be considered [24]. TARC defines the total reflection coefficient of MIMO. The proposed MIMO offers CCL of 0.44 and 0.42 bits/s/Hz and TARC of -20.2 dB and -22.4 dB for resonating frequency. Fig. 16 shows the CCL and TARC for the proposed MIMO. A further important parameter for the MIMO array is mean effective gain (MEG), as shown in Fig. 17. The proposed MIMO provides MEG between -2 to 0 dB.

Table 2 illustrates the parameter specification for the designed single antenna and the proposed MIMO array. This table shows that the performance of the MIMO array is much improved than a single antenna.

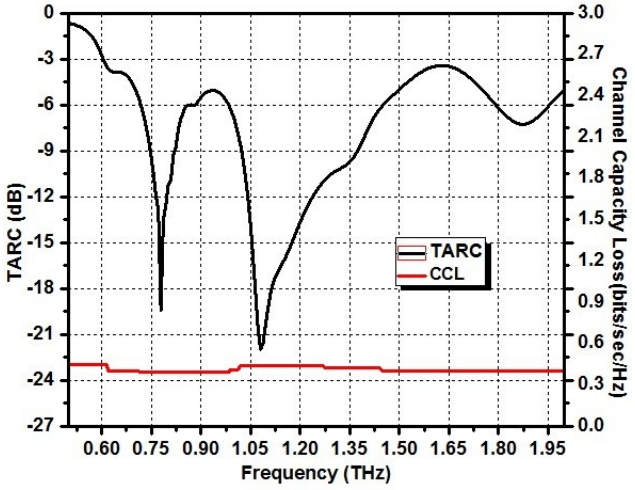

Fig. 16. TARC and CCL of 2×2 MIMO (color online)

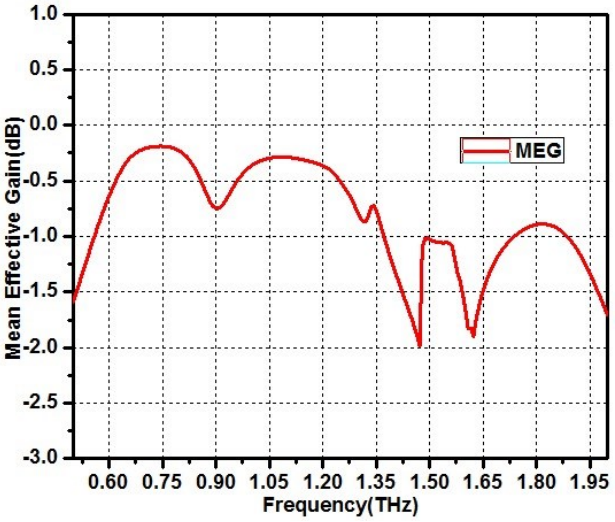

Fig. 17. MEG of 2×2 MIMO (color online)

The electric field (E-field) and magnetic field (F-field) of the proposed MIMO array are illustrated in Figs. 16 and Fig. 17, respectively. Figures show that the maximum current flow occurs at port 1 of the MIMO array which indicates that there is negligible mutual coupling between each four ports. The highest e-field strength for the proposed MIMO is 2.2866e+006 V/m, and the magnetic field strength is 2.7349e+004 A/m.

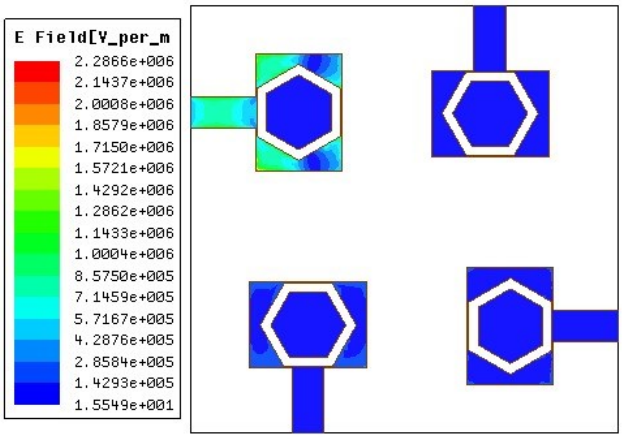

Fig. 18. E-field of 2×2 MIMO (color online)

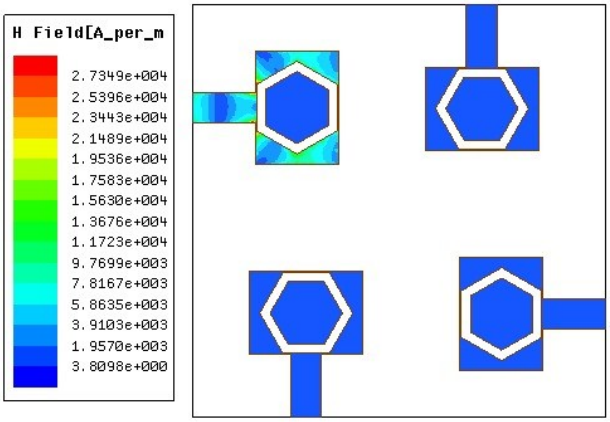

Fig. 19. F-field of 2×2 MIMO (color online)

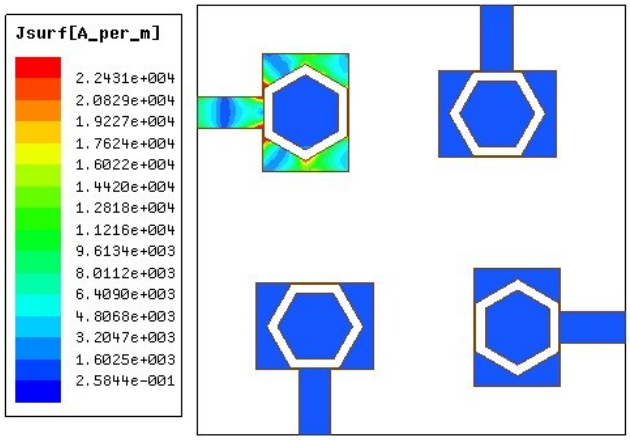

Fig. 20. Surface Current for 2×2 MIMO (color online)

Moreover, Fig. 19 shows the current distribution for the simulated MIMO array. The transmission line and border area of a radiating element have the highest current distribution. The highest current distribution for the proposed MIMO is 2.2431+004 A/m.

Table 2. Proposed single Antenna and MIMO array simulated results

Parameters	Resonating frequency	Reflection Coefficient (dB)	Maximum B.W. (GHz)	Gain (dB)	Directivity (dB)	VSWR	Max. Radiation Efficiency	ECC	Diversity (dB)	CCL (bits/s/Hz)	TARC (dB)
Antenna A	0.7261, 1.0804	-22.8341, -21.1270	81.3, 102.8	7.31	7.32	1.0824, 1.1654	86%	-	-	-	-
Antenna B	0.7638, 1.0879	-28.0939, -25.1371	90.1, 103.9	9.16	9.17	1.0737, 1.1112	88%	-	-	-	-
MIMO Antenna	0.7638, 1.0804	-37.4166, -34.6443	91.9, 170.3	12.30	12.33	1.2280, 1.0786	90%	0.0008	9.9999	0.44, 0.42	-20.2, -22.4

4. Comparison of state-of-the-art

The proposed MIMO antenna for THz applications is compared with the already designed THz antennas in this section Table 3 lists. Among the performance metrics used in the comparison are antenna gain, bandwidth, directivity, radiation efficiency, reflection coefficient, and VSWR. Table 3 indicates that the proposed MIMO Antenna performs better than the earlier suggested THz antennas. The designed MIMO antenna array covers a better gain and directivity. Over the resonant frequency, the proposed MIMO array has excellent antenna bandwidth and consistent radiation output. In addition, many researchers have only developed a single antenna for THZ and have not explained the optimal arrangement for a MIMO array.

Table 3. Performance assessment of the proposed MIMO compared to previously designed antennas for THz

Reference	Resonating Frequency (THz)	Substrate	Return loss (dB)	Max. Bandwidth (GHz)	Peak Gain (dB)	Directivity (dB)	Efficiency (%)	VSWR	Size (L × W × H)µm
[16]	0.658, 0.858	Polyimide	-23.98, -29.29	57.96	8.28	9.8	75	-	400 × 400 × 50
[17]	0.65	Polyimide	-30	40	11.3	-	66.4	-	1200×2200×191
[18]	2.96	Polyimide	-50	26.93	5.40	-	-	1.022	60×60×26
[19]	0.35, 0.58, 0.69	Polyimide	-31.38. -19.31, -60.1	-	7.66	-	88	1.001	260 × 300×35
Proposed massive MIMO antenna array	0.7638, 1.0804	Polyimide	- 37.4166, -34.6443	170.3	12.30	12.33	90	1.2280, 1.0786	440×400×40

5. Conclusion

This research concentrates on dual-band MIMO antenna arrays for THz communication networks. The proposed research offers higher bandwidth, enhanced antenna gain, higher efficiency as well as directivity and low isolation. The proposed MIMO exhibits a return loss of -37.4166 dB and -34.6443dB for the resonating frequencies of 0.7638 THz, and 1.0804 THz, respectively. Moreover, it offers a peak gain of 12.30 dB, a higher directivity of 12.33 dB, a larger bandwidth of 170.3 and a radiation efficiency of 90%. The isolation between the ports is less than -20dB and the VSWR lies between 1 to 2. Moreover, the MIMO parameters such as ECC is 0.0008, diversity gain is 9.9999 dB, TARC is less than -20 dB, MEG is -2 to 0 dB and CCL is 0.44. Because the MIMO must account for the numerous losses for the THz environment, a 2×2 MIMO is analysed and simulated. In the forthcoming technology of wireless networks, the developed MIMO can be considered as a promising contender for various on-chip components.

Acknowledgement

This work has been done with the support of research initiation grant awarded to one of the authors Dr. Simranjit Singh at Punjab Engineering College, Chandigarh, India.

References

[1] Syeda Fizzah Jilani, Alomainy Akram, IET Microwaves, Antennas & Propagation **12**(5), 672 (2018).
[2] Henry Abu Diawuo, Young-Bae Jung, IEEE Antennas and Wireless Propagation Letters **17**(7), 1286 (2018).
[3] R. L. Haupt, Y. Rahmat-Samii, IEEE Antennas and Propagation Magazine **57**(1), 86 (2015).
[4] P. Koundal, S. Singh, R. Kaur, 9th International Conference on Signal Processing and Communication (ICSC), NOIDA, India, 108 (2023).
[5] Z. Chen, Xinying Ma, Bo Zhang, Yaxin Zhang, Zhongqian Niu, Ningyuan Kuang, Wenjie Chen, Lingxiang Li, Shaoqian Li, China Communications **16**(2), 1 (2019).
[6] K. Poonam, S. Simranjit, R. Kaur, Massive MIMO Antenna Array at Terahertz Band for Short-range Communications, Preprint (Version 1) available at Research Square (2023).
[7] Sneha Moghe, Leeladhar Malviya, 2022 IEEE Microwaves, Antennas, and Propagation Conference (MAPCON), 686 (2022).
[8] M. Moussaoui, M. E. Jbari, Advances in Signal and Communication Processing for Ultra-High-Speed Terahertz Communications Terahertz Devices, Circuits and Systems, 289 (2022).
[9] Prapti R. Pandya, M. Sarada Devi, Namrata Langhnoja, Terahertz Antennas–Review and Design, Terahertz Devices, Circuits and Systems: Materials, Methods and Applications, 305 (2022).
[10] J.-B. Tan, L. Dai, IEEE Journal on Selected Areas in Communications **39**(6), 1693 (2021).
[11] Chong Han, A. Ozan Bicen, Ian F. Akyildiz, IEEE Transactions on Signal Processing **64**(4), 910 (2016).
[12] Rohit Yadav, Ajay Parmar, Leeladhar Malviya, Dhiraj Nitnaware, IEEE Indian Conference on Antennas and Propagation (InCAP), 544 (2021).
[13] Kaur Harmeet, Rajandeep Singh, Ramandeep Kaur, Optoelectron. Adv. Mat. **16**(5-6), 193 (2022).
[14] Rashmi Pant, Leeladhar Malviya, International Journal of Communication Systems **36**(8), e5474 (2023).
[15] C. Y. Lin, G. Y. Li, IEEE Communications Magazine **54**(12), 124 (2016).
[16] M. Singh, S. Singh, M. T. Islam, Highly Efficient Ultra-Wide Band MIMO Patch Antenna Array for Short Range THz Applications, Springer eBooks, 193 (2021).
[17] Rashmi Pant, Malviya, Leeladhar, Frequenz **78**, 1 (2024).
[18] S. M. Shamim, T. Youssef, A. Nahid, N. K. Anushkannan, S. D. Umme, H. Md Arafat, I. Nazrul, Optical and Quantum Electronics **55** (7), 618 (2023).
[19] Gaofang Li, Chenguang Huang, Renjie Huang, Bo Tang, Jingguo Huang, Jie Tan, Nenghong Xia, Haoyang Cui, Photonics **11**(4), 307 (2024).
[20] S. Waleed, U. Sadiq, A. Ashfaq, A. A. Nisar, C. Dong-you, Applied Sciences **12**(18), 9231 (2022).
[21] R. K. Kushwaha, P. Karuppanan, L. Malviya, Physica B: Condensed Matter **545**, 107 (2018).
[22] Rohit Yadav, Ajay Parmar, Leeladhar Malviya, Dhiraj Nitnaware, IEEE 11th International Conference on Communication Systems and Network Technologies (CSNT), 26 (2022).
[23] S. Mandeep, S. Simranjit, Photonics and Nanostructures-Fundamentals and Applications **44**, 100900 (2021).
[24] Rashami Pant, Leeladhar Malviya, Indian Conference on Antennas and Propagation (InCAP), Jaipur, India, 68 (2021).

*Corresponding author: poonam5koundal@gmail.com